The Company of **Biologists**

STEM CELLS AND REGENERATION

RESEARCH ARTICLE

TOPLESS mediates brassinosteroid control of shoot boundaries and root meristem development in *Arabidopsis thaliana*

Ana Espinosa-Ruiz[1,‡], Cristina Martínez[1,‡], Miguel de Lucas[1,*], Norma Fàbregas[2], Nadja Bosch[2], Ana I. Caño-Delgado[2] and Salomé Prat[1,§]

ABSTRACT

The transcription factor BRI1-EMS-SUPRESSOR 1 (BES1) is a master regulator of brassinosteroid (BR)-regulated gene expression. BES1 together with BRASSINAZOLE-RESISTANT 1 (BZR1) drive activated or repressed expression of several genes, and have a prominent role in negative regulation of BR synthesis. Here, we report that BES1 interaction with TOPLESS (TPL), via its ERF-associated amphiphilic repression (EAR) motif, is essential for BES1-mediated control of organ boundary formation in the shoot apical meristem and the regulation of quiescent center (QC) cell division in roots. We show that TPL binds via BES1 to the promoters of the *CUC3* and *BRAVO* targets and suppresses their expression. Ectopic expression of TPL leads to similar organ boundary defects and alterations in QC cell division rate to the *bes1-d* mutation, while *bes1-d* defects are suppressed by the dominant interfering protein encoded by *tpl-1*, with these effects respectively correlating with changes in *CUC3* and *BRAVO* expression. Together, our data unveil a pivotal role of the co-repressor TPL in the shoot and root meristems, which relies on its interaction with BES1 and regulation of BES1 target gene expression.

KEY WORDS: BR signaling, BES1, EAR domain, TOPLESS, Organ boundary, Quiescent center, Quiescence

INTRODUCTION

Brassinosteroids (BRs) are steroid plant hormones with an essential role in plant growth and development (Clouse, 2011; Guo et al., 2013). In tight connection with environmental cues and other plant hormones, BRs control shoot and root growth and distinct developmental programs such as photomorphogenesis, organ boundary formation and vascular differentiation (Ibanes et al., 2009; Bell et al., 2012; Gendron et al., 2012; Wang et al., 2012). BR perception triggers a signaling cascade that ultimately leads to activation and accumulation of two homologous transcription factors: BRI1-EMS-SUPPRESSOR 1 (BES1) and BRASSINAZOLE-RESISTANT 1 (BZR1). In the nucleus, BES1 and BZR1 modulate the expression of thousands of genes with a role in cell elongation, BR synthesis, and in the control of multiple cellular processes (He et al., 2005; Yin et al., 2005). Such a wide range of transcriptional

effects relies on the ability of BES1 and BZR1 to interact with different families of transcription factors, which partly modify their DNA-recognition motif and switch their transcriptional activity from a repressor to activation function (Yin et al., 2005; Oh et al., 2012). Although early studies showed that BZR1 binds a conserved BRRE (CGTGC/TG) element in the promoters of BR biosynthetic genes (He et al., 2005), whereas BES1 activates gene expression by recognizing as a complex with the bHLH factor BES1-INTERACTING MYC-LIKE 1 (BIM1) an E-box (CANNTG) element in its target promoters (Yin et al., 2005), more recent studies have established that both factors have similar DNA binding and transcriptional activities (Sun et al., 2010; Yu et al., 2011). BES1 and BZR1 interact with the PHYTOCHROME-INTERACTING FACTOR (PIF) family of bHLH factors to co-regulate a large number of light- and BR-responsive genes (Oh et al., 2012; Bernardo-García et al., 2014), and are blocked by the DELLA repressors via a similar sequestration mechanism as PIFs (Bai et al., 2012; Gallego-Bartolome et al., 2012; Li et al., 2012). However, BES1 and BZR1 also play independent roles in other processes, such as BES1-mediated attenuation of abscisic acid (ABA) signaling (Ryu et al., 2014) and BZR1 negative regulation of immune signaling (Lozano-Durán et al., 2013).

BES1 and BZR1 share a conserved ERF-associated amphiphilic repression (EAR) motif in the C-terminal region, and recent studies show that the repressive function of these factors involves direct interaction with the co-repressor TOPLESS (TPL) (Oh et al., 2014; Ryu et al., 2014). TPL and its TOPLESS-RELATED (TPR) homologs belong to the family of Groucho/Tup1 transcriptional co-repressors (Long et al., 2006), which bind a wide range of transcription factors via their EAR motifs to repress downstream targets (Kagale and Rozwadowski, 2011; Causier et al., 2012). Repression by TPL/TPR has been associated with the recruitment of HISTONE DEACETYLASE 19 and 6 (HDA19 and HDA6), two closely related deacetylases that promote chromatin compaction and transcriptional inactivation (Long et al., 2006; Krogan et al., 2012; Wang et al., 2013). TPL/TPRs regulate gene expression in multiple hormone-response pathways, including auxin, jasmonate and strigolactone, through their interaction with the Aux/IAA, JAZ and SMLX transcriptional repressors (Szemenyei et al., 2008; Pauwels et al., 2010; Wang et al., 2015), in addition to playing a role in the central oscillator through interaction with PRR5, PRR7 and PRR9 (Wang et al., 2013). Likewise, TPL modulates BZR1-regulated cell elongation (Oh et al., 2014) and mediates antagonistic effects of BRs on ABA signaling, a response that is specifically controlled by BES1 (Ryu et al., 2014).

BR signaling is also crucial to the control of cell proliferation in the shoot and root meristems. In the shoot apical meristem (SAM), BRs specifically modulate limited growth of organ boundaries, a group of small rarely dividing cells that separate new forming organs from the meristem (Fletcher, 2002; Reddy et al., 2004;

[1]Department of Plant Molecular Genetics, Centro Nacional de Biotecnología-CSIC, Darwin 3, Madrid E-28049, Spain. [2]Department of Molecular Genetics, Centre for Research in Agricultural Genomics (CRAG) CSIC-IRTA-UAB-UB, Barcelona E-08193, Spain.
*Present address: Department of Biosciences, Durham University, Stockton Road, Durham DH1 3LE, UK.
‡These authors contributed equally to this work

§Author for correspondence (sprat@cnb.csic.es)

S.P., 0000-0003-2684-5485

DEVELOPMENT

Barton, 2010). BZR1 fusions to the fluorescent protein YFP revealed that this factor is depleted in the boundaries, whereas *bzr1-1D*-CFP shows uniform distribution in the SAM and boundary cells (Gendron et al., 2012). BZR1 directly represses expression of the organ boundary identity *CUP-SHAPED COTYLEDON1*, *2* and *3* (*CUC1-3*) genes, with constitutive *bzr1-1D* mutants found to display organ fusion defects indicative of impaired organ boundary separation (Bell et al., 2012; Gendron et al., 2012).

Reduced BR signaling is likewise required to maintain quiescence at the root stem cell niche (Gonzalez-Garcia et al., 2011; Heyman et al., 2013). BRs promote quiescent center (QC) cell division through a cell-autonomous pathway that is independent of auxin and ethylene signaling (Gonzalez-Garcia et al., 2011; Lee et al., 2015) and that is mediated by the R2R3 MYB transcription factor BRASSINOSTEROIDS AT VASCULAR AND ORGANIZING CENTER (BRAVO). *BRAVO* is specifically expressed in the QC and stele initials and maintains QC quiescence downstream from *BRASSINOSTEROID INSENSITIVE 1* (*BRI1*) (Vilarrasa-Blasi et al., 2014).

While recent studies provided evidence of a function of TPL/TPR in BES1/BZR1-mediated control of cell elongation, it is at present unknown whether this family of co-repressors is also involved in the promotion of cell proliferation in response to BR signaling. Here, we show that mutation of the EAR domain in the protein encoded by *bes1-D* reverses both the organ boundary and QC defects of *bes1-D* overexpressors. Increased *TPL* gene dosage aggravates the organ fusion and QC cell division phenotype of *bes1-D* mutants, while overexpression of the protein encoded by *tpl-1* largely overrides *bes1-D* effects. We show that TPL binds to conserved BRRE and G-box elements in the *CUC3* and *BRAVO* promoters through complex formation with BES1, and that *pTPL*::TPL seedlings display similar organ fusion defects and increased QC division rates to *bes1-D* mutants. Together, these results unveil a pivotal role of the co-repressor TPL in BR-regulated expression in the root and shoot meristems, and demonstrate that this function is essential to organ boundary initiation and maintenance, and to the preservation of low QC cell division rates.

RESULTS

BES1-TPL interaction is required for BES1 transcriptional activity

BES1, BZR1 and BEH1-4 all contain a conserved EAR domain (LXLXL) in their C-terminal region. Since EAR domain proteins were identified in complexes with the co-repressor TPL (Kagale et al., 2010), we investigated whether BES1 directly interacts with TPL. We analyzed the interaction of these proteins *in vitro* in a yeast two-hybrid assay and *in vivo* using bimolecular fluorescence complementation (BiFC) and co-immunoprecipitation (co-IP) studies in *Nicotiana benthamiana* leaves. As shown in Fig. S1A, BES1 and TPL were observed to interact in yeast cells, and this interaction is fully dependent on the presence of an intact EAR domain. Fluorescence of the reconstituted split YFP protein was observed in the nucleus of leaf cells co-transfected with the BES1-eYFP[N] and TPL-eYFP[C] constructs, but not in cells expressing PIF4-eYFP[N] and TPL-eYFP[C], which were used as negative controls (Fig. S1B). TPL-HA was also pulled down from leaf extracts co-expressing the BES1-GFP and TPL-HA proteins, after BES1-GFP immunoprecipitation. By contrast, a mutated version of BES1, in which the three Leu residues in the EAR domain were replaced by Ala (BES1-EARm-GFP), was unable to pull down TPL-HA (Fig. S1C), demonstrating that TPL and BES1 interact via the BES1 EAR domain.

To test whether this domain is required for BES1 function, we analyzed repressive activity of the wild-type and BES1-EARm proteins in transient assays, using the *pDWF4*::LUC construct as a reporter. *N. benthamiana* leaves were agro-infiltrated with the *pDWF4*::LUC construct alone, or in combination with *35S* constructs for BES1, bes1-D, BES1-EARm or bes1-D-EARm proteins, and leaf discs were used to measure LUC activity. (Note that we refer here to the protein encoded by *bes1-D* as bes1-D and, likewise, to the protein encoded by *tpl-1* as tpl-1.) As shown in Fig. S2A, expression of the BES1 and bes1-D proteins efficiently repressed the *DWF4* promoter, but this repressive effect was not observed for the BES1-EARm or bes1-D-EARm mutated proteins. Also, expression of the TPL co-repressor reduced LUC activity driven by the *DWF4* promoter and enhanced the repressive effects of BES1 (Fig. S2B), in contrast to a partial reversal of BES1 inhibitory effects observed on expression of the mutant tpl-1 protein. These effects were not observed when TPL or tpl-1 was co-expressed with BES1-EARm, in support of a function of TPL in repressing *DWF4* expression via interaction with the BES1 EAR motif (Fig. S2B).

To confirm these results *in vivo*, we generated *35S*::*bes1-D*-GFP and *35S*::*bes1-D-EARm*-GFP transgenic lines, and two *bes1-D-EARm* lines (L13 and L33) were further characterized (Fig. S3A). As expected, overexpression of the bes1-D-GFP protein phenocopied the *bes1-D* mutant, with a decreased response to the biosynthetic inhibitor brassinazole (BRZ), and the characteristic bent petioles and curled leaves of adult *bes1-D* plants (Fig. S3B-D). However, none of these phenotypes was recapitulated in *bes1-D-EARm*-GFP lines, nor in the stronger overexpressor (Fig. S3B-D), indicating that the EAR domain is essential for BES1 function.

BR biosynthetic gene expression confirmed that mutation of the EAR domain abolishes the ability of bes1-D to repress *CPD*, *DWF4* and *ROT3* genes (Fig. S3E). *IAA19* and *PRE5* gene activation was also impaired in *bes1-D-EARm* lines, suggesting that the EAR domain is not only essential for bes1-D repressive activity but for the transcriptional activation of its target genes. Together, these results establish that the EAR domain is essential for BES1 transcriptional activity, with mutation of this domain inactivating bes1-D function.

Loss of TPL function abolishes the constitutive BR response phenotype of *bes1-D* mutants

TPL and the four TPR Groucho/Tup1 co-repressors were identified by isolation of the temperature-sensitive *tpl-1* mutant, which shows severe apical-basal axis defects and fused cotyledons and, at restrictive temperatures, the replacement of the shoot by an apical root (Long et al., 2006). The *tpl-1* mutation has a semi-dominant character due to the dominant-negative effect of the N176H substitution over the rest of the TPL/TPRs proteins (Long et al., 2006). Inactivation of all five *TPL/TPR* genes is indeed required to recapitulate the *tpl-1* phenotype, identical phenotypic alterations being also observed in lines ectopically expressing *tpl-1* (Wang et al., 2013).

To obtain additional genetic evidence for BES1 and TPL interaction, we generated double *tpl-1* OX;*bes1-D* and TPL;*bes1-D* lines by crossing plants overexpressing the mutant tpl-1 protein (*tpl-1* OX) or which expressed an extra copy of the *TPL* gene (*pTPL*::TPL), respectively, into the *bes1-D* mutant background. As shown in Fig. 1A,B, overexpression of *tpl-1* abolished the BRZ-insensitive phenotype of the constitutive *bes1-D* mutants, with *tpl-1* OX;*bes1-D* seedlings showing shorter hypocotyls than *bes1-D* or the wild type (WT), and a similar growth inhibition response to BRZ as WT
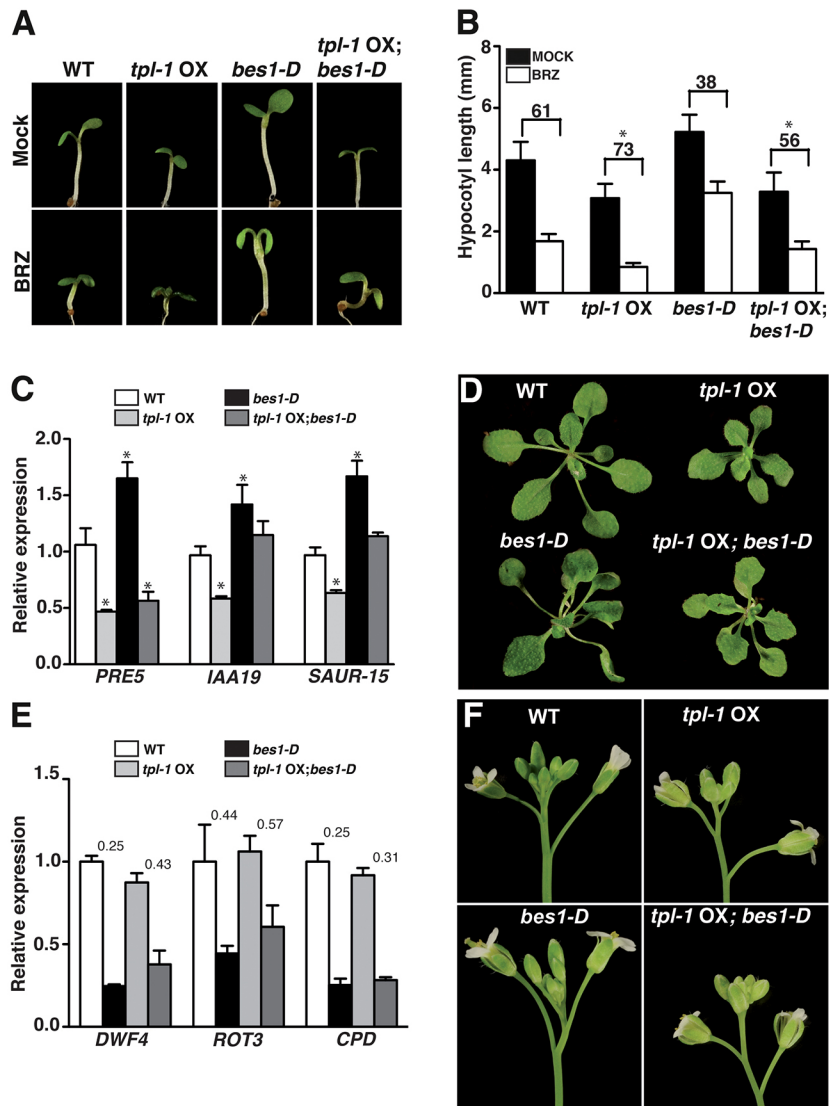
Fig. 1. Characterization of *tpl-1* OX and *tpl-1* OX;*bes1-D* plants. (A) Phenotype of 7-day-old WT, *tpl-1* OX, *bes1-D* and *tpl-1* OX;*bes1-D* seedlings grown under short-day conditions on MS growth medium (mock) or MS medium supplemented with 0.5 µM brassinazole (BRZ). (B) Hypocotyl lengths of seedlings grown in the same conditions as A. Numbers above the bars indicate hypocotyl growth reduction in BRZ media. Asterisks indicate a statistically different response of *tpl-1* OX compared with the corresponding background genotypes ($P<0.01$, Student's *t*-test). Error bars represent s.d. ($n=20$). (C,E) Quantitative real-time PCR analysis of BES1-activated genes (C) and BR biosynthesis BES1-repressed genes (D). Gene expression levels were normalized to *PP2A*. Error bars indicate s.d. ($n=3$ biological replicates). *$P<0.05$ (Student's *t*-test) for each genotype versus WT. Numbers (E) represent relative expression levels. (D,F) Phenotypes of 4-week-old plants (D) and inflorescences (F) of the indicated genotypes.

plants. Expression of this mutant protein caused by itself the inhibition of hypocotyl elongation, and a hypersensitive response to BRZ, indicative of a function of TPL in BR-dependent promotion of hypocotyl growth.

BES1 and BZR1 promote plant growth via direct activation of multiple cell wall remodeling and auxin signaling genes, including *IAA19*, *SAUR15* and *PRE5* (Sun et al., 2010; Oh et al., 2012). Expression of these gene targets was significantly reduced in *tpl-1* OX plants, the tpl-1 protein also suppressing activation of these genes in the *bes1-D* background (Fig. 1C). Moreover, as reported for the *tpl;tpr1;tpr4* triple mutant (Oh et al., 2014), *bes1-D* caused a milder repression of the BR biosynthetic *DWF4*, *ROT3* and *CPD* genes in *tpl-1* OX seedlings than in the WT background (Fig. 1E).

Notably, *tpl-1* overexpression rescues the bent petioles and curly leaf phenotype of adult *bes1-D* plants, with *tpl-1* OX lines showing smaller and more compact rosettes because of their shorter petioles (Fig. 1D). Upon flowering transition, *tpl-1* OX inflorescences were also smaller and more compact than WT, and more detailed phenotypic studies showed that their compact aspect is associated with defects in pedicel elongation. By contrast, *bes1-D* inflorescences were larger than those of WT (Fig. 1E), and had bigger flowers as a result of increased expansion of sepals and petals (Fig. S4). All these phenotypes were rescued by *tpl-1*, the

inflorescences of *tpl-1* OX;*bes1-D* plants being identical to those of *tpl-1* OX plants (Fig. 1E, Fig. S4). Together, these results indicate that impaired TPL function interferes with BES1 transcriptional activity, and abolishes not only BES1 repressive function but also its ability to activate gene expression.

Increased TPL dosage results in organ fusion defects
Lines with an increased TPL dosage due to expression of an extra *TPL* gene copy (*pTPL*::TPL) displayed similar organ fusion defects to *bes1-D* mutants (Fig. 2A,C). Fusion of the cauline leaves and pedicels to the main stem and fused sepals and stamens (Fig. 2A,C) were observed in both *bes1-D* and *pTPL*::TPL lines, suggesting that an excess of TPL or BES1 function interferes with proper organ boundary formation. Similar defects were previously reported in *bzr1-1D* mutants (Gendron et al., 2012), indicating that BES1 and BZR1 redundantly control organ boundary formation.

Boundary cells are characterized by expressing a specific set of genes (Tian et al., 2014), including the *CUC1-3* boundary identity genes. This NAC-type family of transcription factors restricts cellular proliferation and differentiation, and plays a pivotal role in organ separation during both the vegetative and reproductive stages (Takada et al., 2001; Vroemen et al., 2003). *CUC1-3* have overlapping functions in boundary maintenance, as indicated by
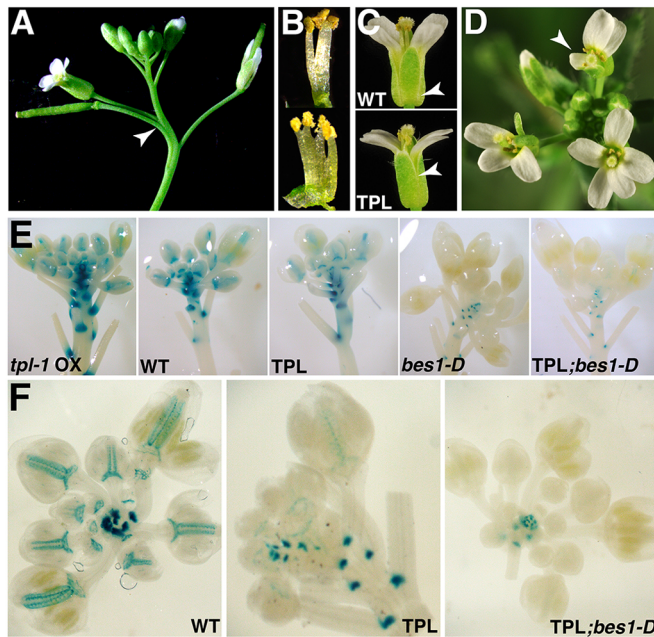
Fig. 2. TPL and BES1 regulate postembryonic organ separation and cooperatively repress *CUC3* expression. (A-D) Defects in organ boundary formation and maintenance observed in *pTPL*::TPL plants (TPL in the figure): pedicel fusion to the stem (A), fused stamens (B), partially fused sepals (C), flowers with three or five petals and petals of different size (D). Arrowheads indicate fused organs. (E) *pCUC3*::GUS expression in the inflorescence and branch junctions of *tpl-1* OX, WT, *pTPL*::TPL (TPL), *bes1-D* and *pTPL*::TPL; *bes1-D* (TPL;*bes1-D*) plants. First primary inflorescences were collected for each genotype and used for staining. (F) Detail showing the boundary-associated pattern of *pCUC3*::GUS expression in WT, TPL and TPL;*bes1-D* inflorescences.

the lack of phenotype of single loss-of-function mutants (Vroemen et al., 2003; Laufs et al., 2004; Hibara et al., 2006; Burian et al., 2015). Likewise, incomplete penetrance of their organ fusion defects suggests that other pathways converge on the control of boundaries (Johnston et al., 2014; Colling et al., 2015; Hepworth and Pautot, 2015).

As for *cuc* mutants, sporadic organ fusion defects such as pedicel-stem fusions (Fig. 2A), fused stamens (Fig. 2B) and partially fused sepals (Fig. 2C) were observed in both *bes1-D* and *pTPL*::TPL plants. Penetrance of this phenotype was similar in *pTPL*::TPL and *bes1-D* plants (2-4%, see Table 1), but was notably increased in the double TPL;*bes1-D* background (11% and 18%, see Table 1), suggesting a cooperative function of the BES1 and TPL proteins in mediating these alterations. Expression of the tpl-1 mutant protein, on the other hand, rescued the organ fusion phenotype of *bes1-D* plants, none of these defects being observed in *tpl-1* OX or *tpl-1* OX;*bes1-D* plants (Table 1).

Table 1. Percentage of flowers that contain stamen-stamen or pedicel-stem fusions

| Genotype	n	Fused stamen (%)	Pedicel-stem fusion (%)
Col-0	151	0 (0)	0 (0)
pTPL::TPL	147	3 (2)	3 (2)
bes1-D	138	6 (4.3)	3 (2.2)
TPL;bes1-D	148	27 (18.2)	17 (11.5)
tpl-1 OX	164	0 (0)	0 (0)
tpl-1 OX;bes1-D	110	0 (0)	0 (0)

A few percent of *bes1-D* (6%) and *pTPL*::TPL (11%) plants displayed floral patterning defects, such as extra petals, or a reduced number of petals of dissimilar size (Fig. 2D, Table S1). A related phenotype has been described for a mutant of *EARLY EXTRA PETALS 1* (*EEP1*), which encodes a microRNA (MIR164c) that post-transcriptionally regulates *CUC1* and *CUC2*, with *eep1* mutants failing to repress *CUC1* and *CUC2* expression in the second whorl (Laufs et al., 2004; Baker et al., 2005). Although *tpl-1* OX rescued the patterning defects of *bes1-D* plants, penetrance of these alterations was not increased in the TPL;*bes1-D* background (Table S1), suggesting that TPL controls petal initiation also via BES1-independent pathways, most likely via regulation of auxin signaling (Szemenyei et al., 2008).

TPL regulates organ separation via BES1-mediated *CUC3* gene repression

To assess whether the fusion defects in *bes1-D* and *pTPL*::TPL lines were associated with downregulation of the *CUC* genes, we examined the spatial pattern of *CUC3* expression in these plants. A *pCUC3*::GUS reporter line (Kwon et al., 2006) was crossed into the *tpl-1* OX, *pTPL*::TPL, *bes1-D* and TPL;*bes1-D* backgrounds and GUS expression was analyzed by staining of the inflorescences (Fig. 2E,F). During floral transition the SAM is converted to an inflorescence meristem. This process involves the formation of meristem-organ boundaries between the central inflorescence meristem and the floral primordia, and organ-organ boundaries that separate the four concentric whorls and adjacent organs within a whorl. *CUC3* is reported to be expressed in each of these boundaries (Vroemen et al., 2003) and, in agreement with previous reports, GUS expression in WT inflorescences was restricted to the adaxial side of the pedicel axils and to the boundaries between floral primordia in the SAM. In floral buds, it formed a ring at the bases of sepals and petals and marked the boundaries between ovule primordia in the gynoecium (Fig. 2F). Notably, *tpl-1* OX increased *CUC3* expression in all these boundary regions, while GUS expression was reduced in both *pTPL*::TPL and *bes1-D* plants. Moreover, TPL;*bes1-D* plants showed an additive inhibition of GUS expression, indicating that TPL and bes1-D synergistically suppress the *CUC3* gene (Fig. 2E,F).

In paraclade junctions between primary and secondary stems *CUC3* expression was restricted to the bases of the cauline leaf and the emerging axillary shoot (Fig. 3B). GUS activity was strongly reduced in *bes1-D* mutants, correlating with defective axillary branch separation (Fig. 3A,B). Reduced GUS expression was likewise detected in *pTPL*::TPL lines, in contrast to *tpl-1* OX which showed an expanded area of *CUC3* expression (Fig. 3B). Also, increased TPL dosage resulted in stronger *CUC3* inhibition and more severe cauline leaf-branch fusions in TPL;*bes1-D* plants, whereas *tpl-1* OX alleviated the fusion defects of *bes1-D* mutants (Fig. 3C). Similar trends in *CUC3* expression were observed by RT-qPCR analyses of young seedlings, with reduced *CUC3* transcript levels detected in *bes1-D*, *pTPL*::TPL and TPL;*bes1-D* lines, whereas in the *tpl-1* OX;*bes1-D* and *bes1-D-EARm* backgrounds expression levels were similar to the WT (Fig. 3E). In these analyses, *CUC3* levels in *tpl-1* OX seedlings were slightly lower than in the WT, which was likely to be due to the delayed leaf differentiation in this genotype. Altogether, these results demonstrate that TPL and BES1 act in concert to repress *CUC3* expression, with impaired TPL function in *tpl-1* overexpressors abolishing *bes1-D*-mediated suppression of *CUC3*.

TPL is recruited to specific DNA promoter regions through interaction with different families of DNA-binding transcription
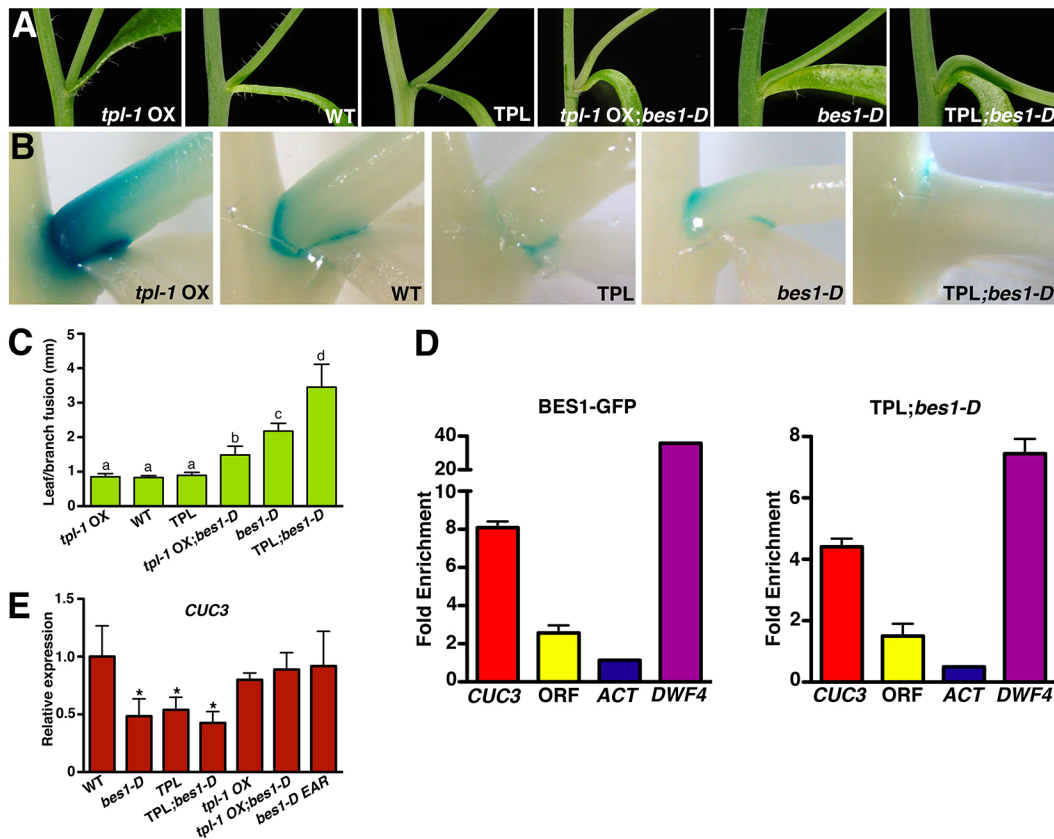
Fig. 3. TPL and BES1 control leaf-branch separation and bind the *CUC3* promoter. (A) Junction between the main stem, axillary branch and cauline leaf in the indicated phenotypes. (B) Detail showing *pCUC3*::GUS expression in the stem-branch junction of the indicated genotypes. (C) Length of fused region between the branch and the cauline leaf. Measurements were made on the lowest cauline leaf axil of plants of the same age (*n*=20). Lowercase letters indicate significant differences by Tukey's multiple comparison test (*P*<0.01). (D) ChIP-qPCR analysis of BES1 and TPL binding to the *CUC3* promoter region. *DWF4* is included as a positive control, and the ORF of *CUC3* (yellow) and *ACT* as negative controls. The experiment was repeated three times with similar results. (E) Quantitative real-time PCR analysis of *CUC3* expression. RNA was extracted from 6-day-old seedlings grown under long-day conditions. Gene expression levels were normalized to those of *PP2A*. Error bars indicate s.d. (*n*=3 biological replicates). *P<0.05 (Student's *t*-test) compared with WT.

factors. To test if TPL binds the same *CUC3* promoter elements as BES1, we performed chromatin immunoprecipitation (ChIP) assays using both *35S*::BES1-GFP plants and transgenic lines expressing the *pTPL*::TPL construct in the *bes1-D* mutant background. BES1-GFP ChIP-PCR studies confirmed that BES1 binds the *CUC3* and *DWF4* promoters with similar affinities, and associates with the same *CUC3* promoter region as BZR1 (Fig. 3D) (Gendron et al., 2012). These two promoter fragments were also enriched by TPL-HA, although binding to the BES1 recognition sites was less efficient than for BES1-GFP (Fig. 3D), consistent with an indirect association of TPL with DNA. Together, these results demonstrate that BES1 recruits the TPL protein to the *DWF4* and *CUC3* promoters, pointing to a pivotal function of the TPL-BES1 module in the control of organ boundary maintenance through direct repression of the *CUC1-3* genes.

TPL modulates root meristem organization through BES1-mediated suppression of *BRAVO*

Reduced BR signaling is crucial to the control of cell cycle progression in the root stem cell niche and to the correct organization of the meristem, whereas increased BR signaling promotes cell elongation and differentiation in the root transition-elongation zone (Gonzalez-Garcia et al., 2011; Chaiwanon and Wang, 2015). The BAS1 and SOB7 BR catabolic enzymes are expressed in the root cap and reduce availability of bioactive BRs in

the adjacent stem cell niche (Chaiwanon and Wang, 2015). In the QC, BR signaling targets the *BRAVO* and *ETHYLENE RESPONSE FACTOR 115* (*ERF115*) factors, which regulate QC quiescence in opposite ways (Heyman et al., 2013; Vilarrasa-Blasi et al., 2014). BRAVO is expressed in the QC and stele initials and acts as a cell-specific repressor of QC division (Vilarrasa-Blasi et al., 2014). *BRAVO* is a repression target of BES1 and BZR1, with reduced expression of this gene in *bes1-D* and *bzr1-1D* mutants leading to ectopic activation of QC division (Vilarrasa-Blasi et al., 2014; Chaiwanon and Wang, 2015). BRAVO also physically interacts with and inactivates BES1, this negative-feedback loop enabling high levels of *BRAVO* expression in QC cells, at the same time that prevents its suppression as a result of fortuitous activation of BR signaling (Vilarrasa-Blasi et al., 2014).

To assess whether TPL function is required for BR-mediated control of cell progression in the root meristem, we examined QC cell division in *pTPL*::TPL and *tpl-1* OX roots. As shown in Fig. 4, expression of an extra *TPL* copy notably increased the number of plants with a divided QC, two QC cell layers being observed in 25% of *pTPL*::TPL roots as compared with 5% in WT roots. By contrast, no QC cell divisions were observed in any of the *tpl-1* OX roots analyzed. Moreover, *pTPL*::TPL expression greatly increased the frequency of divided QC cells in *bes1-D* plants, a double QC layer or partially duplicated cells being seen in 90% of TPL;*bes1-D* roots (Fig. 4). Lines expressing *bes1-D-EARm*, on the other hand,
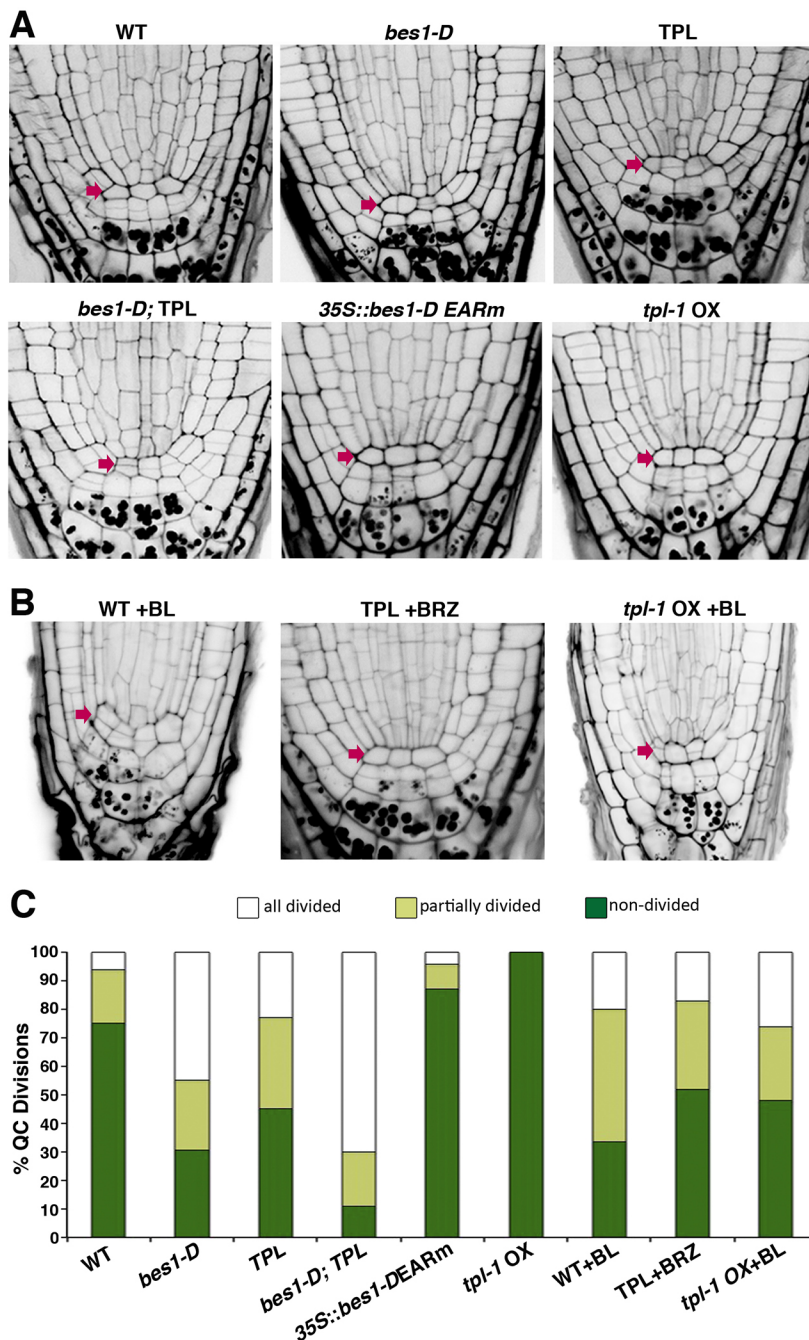
Fig. 4. TPL regulates QC cell division. (A,B) Microscopy images of mPS-PI stained 6-day-old root tips of the indicated genotypes, grown in long-day conditions on MS medium (A) and MS medium supplemented with 0.4 nM BL or 1 µM BRZ (B). Arrows mark QC position. The *35S::bes1-D-EARm* line is L33. (C) Quantification of QC cell divisions expressed as percentage (*n*>50 seedlings for each genotype).

displayed a WT behavior, indicating that the EAR domain is required for BES1 promotion of QC cell division (Fig. 4A,C). To further prove that TPL and *tpl-1* OX effects on QC division depend on BR signaling, we tested whether altered QC division in these genotypes could be rescued by the brassinosteroid 24-epibrassinolide (BL) or BRZ application. As shown in Fig. 4B,C, increased QC division rates were observed in *tpl-1* OX roots upon BL treatment, although divided cells were still less frequent than in the WT, while the increased QC division phenotype of TPL roots was partially rescued by the inhibitor BRZ. Hence, altogether these results are consistent with a cooperative action of BES1 and TPL in promoting QC cell division.

We next analyzed whether TPL effects on QC cell division correlate with suppressed *BRAVO* expression by crossing *pBRAVO*::GFP reporter lines into the *pTPL*::TPL and *tpl-1* OX backgrounds.

Unfortunately, *pBRAVO*::GFP was silenced in *tpl-1* OX lines and we were unable to examine *tpl-1* effects on the expression of this gene. However, a notable decrease in GFP activity was observed in *pTPL*::TPL lines, providing evidence that an increased TPL dosage leads to *BRAVO* suppression (Fig. 5A). Owing to increased QC division, these plants displayed disorganized root meristems (Fig. 5A), and this phenotype was reverted by BRZ application (Fig. 5A,B). Western blot studies of *pBRAVO*::GFP and *pBRAVO*::GFP;TPL roots confirmed that TPL causes a similar reduction in *BRAVO* expression as seen in the WT in response to BL. In addition, BL further suppressed *BRAVO* expression in *pTPL*::TPL roots (Fig. 5C), suggesting an additive effect of TPL and BL in *BRAVO* suppression.

Finally, we tested whether TPL is recruited to the *BRAVO* promoter by performing ChIP-PCR studies on TPL;*bes1-D* lines.
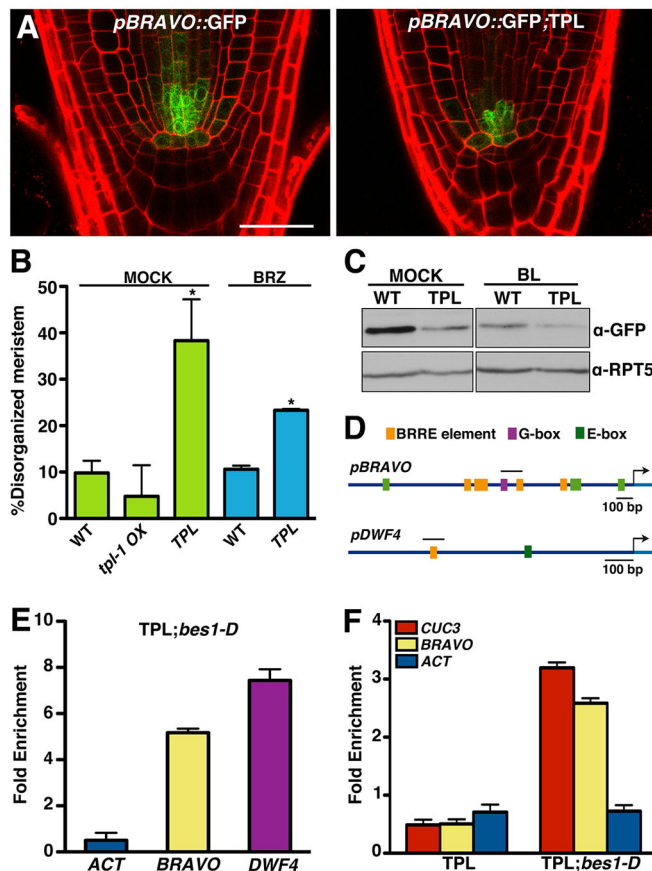
Fig. 5. TPL and BES1 repress *BRAVO* expression. (A) Microscopy images of propidium iodide-stained root tips of 6-day-old WT and *pTPL*::TPL (TPL) seedlings showing *pBRAVO*::GFP expression in QC cells and stele initials. Scale bar: 30 µm. (B) Percentage of roots with disorganized meristems of the indicated genotypes. Seedlings were grown on MS medium for 4 days and 2 additional days on MS medium (mock) or MS medium with 0.5 µM BRZ. Error bars represent ±s.d. (*n*>15). *P<0.05 (Student's *t*-test) for TPL versus WT in mock and for TPL in mock versus BRZ. (C) Western blot showing *pBRAVO*:: GFP expression levels in WT and TPL roots. Hybridization with an anti-RPT5 antibody is included as a loading control. (D) Schematic representation of the *BRAVO* and *DWF4* promoter regions showing the putative BES1/BZR1 binding elements. Bar indicates the region selected for qPCR analysis. (E) ChIP-qPCR assay showing binding of TPL to the *BRAVO* promoter region indicated in D. Six-day-old *pTPL*::TPL;*bes1-D* (TPL;*bes1-D*) seedlings were used for the assay. *DWF4* amplification is included as a positive control and the *ACTIN* ORF (*ACT*) as a negative control. Error bars indicate s.d. (F) ChIP-qPCR assay showing differences in binding of TPL to the *CUC3* and *BRAVO* promoters in *pTPL*::TPL (TPL) compared with TPL;*bes1-D* plants. Six-day-old seedlings grown in 0.5 µM BRZ were used. Experiments were repeated twice with similar results. Error bars indicate s.d. F represents one of the two biological replicates.

BRAVO contains a G-box and several BRRE elements in its 2.1 kb upstream region (Fig. 5D), and significant enrichment was observed for a promoter fragment including the G-box and one of the BRRE elements, previously shown to be recognized by BES1 (Vilarrasa-Blasi et al., 2014), indicating that TPL is recruited to this promoter region by BES1 (Fig. 5E). Additionally, ChIP-PCR experiments on *pTPL*::TPL and TPL;*bes1-D* seedlings grown on BRZ showed that BRZ impaired TPL binding to the *BRAVO* and *CUC3* promoters in *pTPL*::TPL plants, but not in the BRZ-insensitive TPL;*bes1-D* background (Fig. 5F), establishing that BES1 is required for TPL recruitment to these promoters.

Altogether, our results demonstrate that interaction with TPL via its conserved EAR domain is essential for BES1 function in promoting QC cell division, and show that BL effects on QC division depend to a large extent on direct repression of the *BRAVO* gene by BES1. Thus, these data unveil a novel cell-specific function of TPL in the root stem cell niche.

DISCUSSION
BES1 is a pivotal factor in BR signaling, with dual roles as transcriptional activator and repressor. Here, we show that the BES1 EAR domain is essential for its transcriptional activity, and that this conserved domain mediates interaction with the co-repressor TPL, consistent with recent reports (Oh et al., 2014; Ryu et al., 2014).

Notably, overexpression of the mutant tpl-1 protein caused derepression of BES1/BZR1-repressed targets, such as *DWF4*, *ROT3* and *CPD*, and impaired activation of the induced *PRE5*, *IAA19* and *SAUR15* targets (Fig. 1C,E), suggesting that TPL is also required for BES1/BZR1 transcriptional activation functions. This effect was more evident in *tpl-1* OX;*bes1-D* plants, in which *tpl-1* partially suppressed constitutive activation of these targets, in particular of *PRE5*. *tpl-1* OX plants in fact showed shorter hypocotyls and petioles than WT and displayed a hypersensitive response to BRZ, while tpl-1 suppressed the BRZ-insensitive phenotype of *bes1-D* mutants, suggesting that the dominant-negative function of tpl-1 impairs the BR response.

Recent determination of the TOPLESS domain (TPD) crystal structure showed that the N176H substitution in tpl-1 is not relevant in dimerization or EAR binding (Ke et al., 2015). Although the molecular basis for the dominant nature of this mutation is not well understood, our finding that *tpl-1* interferes with BES1 target gene activation suggest that TPL is implicated both in BR-repressed and -activated gene expression. Related findings were also obtained by fusion of the bes1-D-mEAR protein to SRDX, TPL or HDA19 (Ryu et al., 2014), which restitutes constitutive BR signaling activity of the protein and leads to elongated hypocotyl growth on BRZ, thus further supporting of a function of TPL in BES1/BZR1 target gene activation.

A role for TPL in shoot meristem maintenance has been previously reported through its interaction with the WUSCHEL (WUS) homeodomain and RAMOSA1 zinc-finger transcription factors (Kieffer et al., 2006; Sablowski, 2007; Yadav et al., 2011; Gavallotti et al., 2010). Here, we provided biochemical and genetic evidence for a function of the BES1-TPL complex in direct suppression of the *CUC3* and *BRAVO* genes, which act as cell-specific repressors of cell proliferation in the meristem boundaries and the root QC. We showed that increased TPL dosage causes similar organ fusion and QC division alterations as the constitutive BR response *bes1-D* mutation. Moreover, TPL and *bes1-D* have synergistic effects in inhibiting boundary formation and QC quiescence, whereas *tpl-1* expression abolishes *bes1-D* defects. Our findings show that BES1 recruits TPL to the *CUC3* and *BRAVO* promoters to repress boundary and QC cell-specific expression of these genes.

Comparative analyses of BR-responsive gene expression and organ boundary-specific transcriptomes (Tian et al., 2014) provided evidence of a significant overlap between boundary-enriched transcripts and BR signaling-repressed genes (Fig. S5). Most of the BR-repressed transcription factors were reported as BES1 and/or BZR1 direct targets, suggesting that BES1 and BZR1 modulate the expression of other boundary-specific regulators in addition to *CUC* genes. Interestingly, similar comparative studies of the QC cell transcriptome showed that the only transcription factors targeted by BZR1 and repressed by BL were the *BRAVO*, *MONOPOLE* and

PLETHORA genes (*PLT1*, *BABY BOOM/PLT4*) (Chaiwanon and Wang, 2015), supporting a key function of BRAVO downstream of BES1/BZR1 in the root QC.

Reduced division of boundary cells is crucial to the separation of young organs from the central meristem, and to the maintenance and organization of the meristem. Boundary cells express a specific set of genes that restrict cell division and auxin efflux carrier activity while promoting meristematic gene expression (Hepworth and Pautot, 2015). These cells, similar to the root QC, function as a type of organizing center, regulating the patterning and development of adjacent organs (Žádníková and Simon, 2014; Yu and Huang, 2016), thus highlighting a pivotal role of TPL in the organization of the shoot and root meristems. Consistent with this function, TPL is expressed at higher levels in the SAM and root meristem zone, and in young actively dividing tissues (Fig. S6). Moreover, our results provide evidence for a prevalent function of the BES1/BZR1-TPL module in coordinating the balance between cell proliferation and differentiation in both the root meristem and shoot boundary domains, therefore linking organogenesis to the maintenance of meristem activity.

A further intriguing question is why TPL activity is required for the activation function of BES1 and BZR1. Groucho/Tup1 co-repressors are believed to function as binding scaffolds for histone deacetylases and chromatin remodeling complexes (Long et al., 2006; Zhu et al., 2010; Krogan et al., 2012), but their exact mechanism of action is not yet understood. Although genetic evidence suggests that TPL acts through HDA19 (Long et al., 2006), high-throughput yeast two-hybrid approaches failed to identify HDA19 as a direct TPL interactor (Causier et al., 2012), whereas interaction of these proteins was observed in plant extract pulldown experiments (Zhu et al., 2010). This would indicate that additional factors bridge TPL and HDA19 and, in fact, yeast two-hybrid studies showed that TPL/TPR directly bind PKR1, a homolog of the PICKLE [PKL; ENHANCED PHOTOMORPHOGENIC 1 (EPP1)] chromatin remodeling factor (Causier et al., 2012). Interestingly, PKL was recently shown to associate with PIF3 and BZR1, which recruit this chromatin-remodeling factor to the promoters of the *IAA19* and *PRE1* genes (Zhang et al., 2014). Thus, it is possible that TPL forms chromatin modification complexes with opposite transcriptional outputs depending on its interaction with BES1 or the BES1-PIF heterodimer, an important task for the future being the identification of such complexes.

MATERIALS AND METHODS
Plant materials and growth conditions
tpl-1 OX, *pTPL*::TPL (Wang et al., 2013), *pCUC3*::GUS (Kwon et al., 2006) and *pTPL*::GUS (Tao et al., 2013) genotypes are in the *Col*-0 background. *tpl-1* OX and *pTPL*::TPL plants were crossed to the *bes1-D* mutant (introgressed into *Col*-0; Ibanes et al., 2009) to obtain TPL;*bes1-D* and *tpl-1* OX;*bes1-D*, respectively.

Seeds were surface-sterilized for 15 min in 70% (v/v) ethanol and 0.01% (v/v) Triton X-100, followed by two washes of 2 min each in 96% (v/v) ethanol. Air-dried seeds were then sown on half-strength MS agar plates with 1% sucrose and stratified for 3 days at 4°C in the dark. BL (24-epibrassinolide, Sigma-Aldrich) and brassinazole (BRZ, Tokyo Chemical Industry) treatments were performed at 1.0 µM and 0.8 µM, respectively. Hypocotyls were measured using ImageJ (NIH) software.

Plasmid constructs
Full-length coding regions for the *Arabidopsis* BES1, TPL and PIF4 proteins were amplified with primers BES1-F/BES1-R, TPL-F/TPL-R and PIF4-YFP-F/PIF4-YFP-R, respectively (Table S2). The *bes1-D* mutant ORF was amplified from an *Arabidopsis bes1-D* mutant cDNA using

primers BES1-F and BES1-R. To obtain the BES1-EARm and *bes1-D*-EARm constructs, primers BES1-F and BES1-EARm-R (Table S2) were used to introduce the EAR mutation into the corresponding ORFs, using as a template wild-type and *bes1-D* cDNA, respectively. The PCR-amplified fragments were cloned into pENTR/D-TOPO (Invitrogen) and used for subsequent LR reactions.

BES1, BES1-EARm, *bes1-D* and *bes1-D-EARm* full-length coding regions were cloned by LR clonase (Invitrogen) recombination into pGWB5 (Nakagawa et al., 2007) to obtain the *35S*::BES1-GFP, *35S*::BES1-EARm-GFP, *35S*::*bes1*-D-GFP and *35S*::*bes1*-D-EARm-GFP constructs.

The TPL coding region was inserted by LR clonase recombination into pGWB14 (Nakagawa et al., 2007) to create the *35S*::TPL-HA binary vector.

The *DWF4* promoter region was amplified using primers pDWF4-F and pDWF4-R (Table S2) and cloned into LucTrap-3 (Calderón-Villalobos et al., 2006) to obtain the *pDWF4*::LUC reporter plasmid.

Transgenic plants
35S::*bes1-D*-GFP and *35S*::*bes1-D-EARm*-GFP constructs were transformed into the *Agrobacterium tumefaciens* strain GV3101. *Arabidopsis* transformation was performed through the floral dip method. Homozygous *Arabidopsis* lines were identified by kanamycin resistance and lines with appropriate expression of the transgene selected by western blot immunodetection using an anti-GFP antibody (Roche, 11 814 460 001).

Bimolecular fluorescence complementation assay (BiFC)
The TPL, PIF4 and BES1 coding sequences were inserted by LR reaction (Invitrogen) into pBiFC binary vectors containing the N-terminal and C-terminal YFP fragments (YFPN43 and YFPC43, respectively). Plasmids were transformed into the *A. tumefaciens* GV3101 strain and infiltrated into *N. benthamiana* leaves. The p19 protein was used to suppress gene silencing. Two days after infiltration, leaves were observed under a Leica TCS SP5 laser scanning confocal microscope.

Co-immunoprecipitation
N. benthamiana leaves were co-infiltrated with *Agrobacterium* cultures bearing the *35S*::BES1-GFP, *35S*::BES1-EARm-GFP and *35S*::TPL-HA plasmids in the appropriate combinations. After 48 h, leaves were homogenized in protein extraction buffer: 20 mM Tris-HCl pH 7.5, 5 mM MgCl$_2$, 75 mM NaCl, 2.5 mM EDTA, 25 mM β-glycerophosphate, 0.1% Nonidet P-40, 10 mM NaF, 0.05% sodium deoxycholate, 5 mM β-mercaptoethanol, 10 µM MG-132, 1 mM PMSF and protease inhibitors (Roche). Extracts were cleared by centrifugation at 13,000 *g* for 15 min at 4°C, and 1 ml of the supernatant was incubated at 4°C for 3 h with 50 µl anti-GFP magnetic beads (µMACS Epitope Tag, Miltenyi Biotec). Beads were bound using a magnet and washed five times with 500 µl extraction buffer. Immunocomplexes were eluted by boiling for 2 min in 50 µl 2× SDS loading buffer. Anti-HA-peroxidase (Roche, 11 867 423 001) and anti-GFP-peroxidase (Miltenyi Biotec, 130-091-833) antibodies were used for immunodetection.

Yeast two-hybrid assay
Yeast two-hybrid assays were performed with the GAL4 Two-Hybrid System (Clontech). The complete ORFs of the TPL, BES1 and BES1-EARm proteins were introduced by LR clonase recombination into the pGADT7 and pGBKT7 Gateway-compatible vectors (Clontech). The NINJA-pGBT9 plasmid was a kind gift from Dr Roberto Solano (CNB-CSIC). Appropriate plasmid combinations were transformed into the yeast strain AH109 by the lithium acetate method and reporter gene activation was assayed by selection on SD-LWHA plates.

Luciferase activity assays
N. benthamiana leaves were co-infiltrated with *A. tumefaciens* cultures bearing the *pDWF4*::LUC reporter construct, alone or in combination with *35S*::BES1-GFP, *35S*::BES1-EARm-GFP, *35S*::*bes1-D*-GFP or the *35S*::*bes1-D-EARm*-GFP effector constructs. Two days after inoculation, 0.5 cm diameter leaf discs were collected and transferred to 96-well microtiter

plates filled with 165 µl 0.5× MS liquid media and 35 µl 1× D-Luciferin substrate (20 µg/ml). At least 12 discs were measured per sample. Luciferase activity was measured with the LB 960 Microplate Luminometer Center using MikroWin software (Berthold).

Quantitative RT-PCR analysis

Total RNA was extracted from whole seedlings using the High Pure Isolation kit (Roche). 1 µg RNA was used for first-strand cDNA synthesis using SuperScript II Reverse Transcriptase (Invitrogen). 1 µl of the cDNA reaction was used for quantitative PCR using the FastStart Universal SYBR Green Master Mix (Roche) and a 7500 Real-Time PCR System (Applied Biosystems), following the manufacturer's instructions. Expression levels were calculated relative to the *PP2A* gene, using the $\Delta\Delta$ threshold cycle (Ct) method (Applied Biosystems). Primers used are listed in Table S2. Results correspond to three biological replicates.

GUS staining

Freshly harvested plant material was placed in cold 90% acetone for 20 min, washed once with water and transferred to staining solution (50 mM NaHPO$_4$ buffer pH 7.2, 2 mM potassium ferricyanide, 2 mM potassium ferrocyanide, 2 mM X-glucuronide, 0.2% Triton X-100). After 5 min vacuum infiltration, samples were placed at 37°C overnight. Next day, they were incubated for 30 min in 20%, 30% and 50% ethanol, fixed in FAA (50% ethanol, 5% formaldehyde, 10% acetic acid) and kept in 70% ethanol until visualization with a stereomicroscope.

Chromatin immunoprecipitation assays

ChIP assays were performed as described previously (Lee et al., 2007). 3 g of 6-day-old *Col*-0, *35S*::BES1-GFP and *pTPL*::TPL-HA;*bes1-D*-GFP seedlings were used for chromatin preparation. The chromatin pellet was sonicated at 4°C with a Diagenode Bioruptor to achieve an average DNA fragment size of ~0.3-0.8 kb. 1 µl anti-GFP (MBL, 598), 1 µl anti-HA (purified in house; 2.2 µg) and 10 µl protein G coupled to magnetic beads (Invitrogen) were used for ChIP. DNA was purified using the MiniElute Reaction CleanUp Kit (Qiagen). An aliquot of untreated sonicated chromatin was reverse cross-linked and used as input DNA control for PCR amplification. Primers used are listed in Table S2.

Confocal microscopy

Analysis of QC cell division rates and visualization of columella cell starch granules were carried out by imaging fixed stained primary roots obtained through a modified pseudoSchiff-propidium iodide (mPS-PI) staining method (Truernit and Haseloff, 2008). For *in vivo* imaging experiments, roots were stained in 10 µg/ml propidium iodide for 1 min, rinsed and mounted in distilled water. A Leica TCS SP5 laser scanning confocal microscope with an excitation beam splitter TD 488/561/633 and an emission band width between 495 and 556 nm was used to visualize the samples. Dividing cells in the QC were manually counted from confocal stacks.

Western blot analysis

Seedlings or roots were homogenized in extraction buffer: 1× PBS, 0.1% SDS, 0.1% Triton X-100, 100 µM PMSF, 5 µM β-mercaptoethanol and protease inhibitors (Roche). Extracts were cleared by centrifugation at 13,000 rpm (17,900 *g*) for 15 min, and the protein concentration determined by Bradford assay (Bio-Rad). Protein samples were boiled in 2× SDS loading buffer and loaded on 8% SDS-PAGE gels. Blots were probed with anti-GFP antibody (Roche) and peroxidase-conjugated secondary antibody (Amersham, NA931V). Anti-RPT5 was used as a loading control.

References

Bai, M.-Y., Shang, J.-X., Oh, E., Fan, M., Bai, Y., Zentella, R., Sun, T.-P. and Wang, Z.-Y. (2012). Brassinosteroid, gibberellin and phytochrome impinge on a common transcription module in Arabidopsis. *Nat. Cell Biol.* **14**, 810-817.

Baker, C. C., Sieber, P., Wellmer, F. and Meyerowitz, E. M. (2005). The early extra petals1 mutant uncovers a role for microRNA miR164c in regulating petal number in Arabidopsis. *Curr. Biol.* **15**, 303-315.

Barton, M. K. (2010). Twenty years on: the inner workings of the shoot apical meristem, a Developmental dynamo. *Dev. Biol.* **341**, 95-113.

Bell, E. M., Lin, W.-C., Husbands, A. Y., Yu, L., Jaganatha, V., Jablonska, B., Mangeon, A., Neff, M. M., Girke, T. and Springer, P. S. (2012). Arabidopsis lateral organ boundaries negatively regulates brassinosteroid accumulation to limit growth in organ boundaries. *Proc. Natl. Acad. Sci. USA* **109**, 21146-21151.

Bernardo-García, S., de Lucas, M., Martínez, C., Espinosa-Ruiz, A., Davière, J.-M. and Prat, S. (2014). BR-dependent phosphorylation modulates PIF4 transcriptional activity and shapes diurnal hypocotyl growth. *Genes Dev.* **28**, 1681-1694.

Burian, A., Raczyńska-Szajgin, M., Borowska-Wykręt, D., Piatek, A., Aida, M. and Kwiatkowska, D. (2015). The CUP-SHAPED COTYLEDON2 and 3 genes have a post-meristematic effect on Arabidopsis thaliana phyllotaxis. *Ann. Bot.* **115**, 807-820.

Calderon-Villalobos, L. I., Kuhnle, C., Li, H., Rosso, M., Weisshaar, B. and Schwechheimer, C. (2006). LucTrap vectors are tools to generate luciferase fusions for the quantification of transcript and protein abundance in vivo. *Plant Physiol.* **141**, 3-14.

Causier, B., Ashworth, M., Guo, W. and Davies, B. (2012). The TOPLESS interactome: a framework for gene repression in Arabidopsis. *Plant Physiol.* **158**, 423-438.

Chaiwanon, J. and Wang, Z.-Y. (2015). Spatiotemporal brassinosteroid signaling and antagonism with auxin pattern stem cell dynamics in Arabidopsis roots. *Curr. Biol.* **25**, 1031-1042.

Clouse, S. D. (2011). Brassinosteroid signal transduction: from receptor kinase activation to transcriptional networks regulating plant development. *Plant Cell* **23**, 1219-1230.

Colling, J., Tohge, T., De Clercq, R., Brunoud, G., Vernoux, T., Fernie, A. R., Makunga, N. P., Goossens, A. and Pauwels, L. (2015). Overexpression of the Arabidopsis thaliana signalling peptide TAXIMIN1 affects lateral organ development. *J. Exp. Bot.* **66**, 5337-5349.

Fletcher, J. C. (2002). Shoot and floral meristem maintenance in Arabidopsis. *Annu. Rev. Plant Biol.* **53**, 45-66.

Gallego-Bartolome, J., Minguet, E. G., Grau-Enguix, F., Abbas, M., Locascio, A., Thomas, S. G., Alabadi, D. and Blazquez, M. A. (2012). Molecular mechanism for the interaction between gibberellin and brassinosteroid signaling pathways in Arabidopsis. *Proc. Natl. Acad. Sci. USA* **109**, 13446-13451.

Gavalloti, A., Long, J. A., Stanfield, S., Yang, X., Jackson, D., Volbrecht, E. and Schmidt, R. (2010). The control of axillary meristem fate in the maize ramosa pathway. *Development* **137**, 2849-2856.

Gendron, J. M., Liu, J.-S., Fan, M., Bai, M.-Y., Wenkel, S., Springer, P. S., Barton, M. K. and Wang, Z.-Y. (2012). Brassinosteroids regulate organ boundary formation in the shoot apical meristem of Arabidopsis. *Proc. Natl. Acad. Sci. USA* **109**, 21152-21157.

Goda, H., Sawa, S., Asami, T., Fujioka, S., Shimada, Y. and Yoshida, S. (2004). Comprehensive comparison of auxin-regulated and brassinosteroid-regulated genes in Arabidopsis. *Plant Physiol.* **134**, 1555-1573.

Gonzalez-Garcia, M.-P., Vilarrasa-Blasi, J., Zhiponova, M., Divol, F., Mora-Garcia, S., Russinova, E. and Caño-Delgado, A. I. (2011). Brassinosteroids

control meristem size by promoting cell cycle progression in Arabidopsis roots. *Development* **138**, 849-859.

Guo, H., Li, L., Aluru, M., Aluru, S. and Yin, Y. (2013). Mechanisms and networks for brassinosteroid regulated gene expression. *Curr. Opin. Plant Biol.* **16**, 545-553.

He, J.-X., Gendron, J. M., Sun, Y., Gampala, S. S. L., Gendron, N., Sun, C. Q. and Wang, Z.-Y. (2005). BZR1 is a transcriptional repressor with dual roles in brassinosteroid homeostasis and growth responses. *Science* **307**, 1634-1638.

Hepworth, S. R. and Pautot, V. A. (2015). Beyond the divide: boundaries for patterning and stem cell regulation in plants. *Front. Plant Sci.* **6**, 1052.

Heyman, J., Cools, T., Vandenbussche, F., Heyndrickx, K. S., Van Leene, J., Vercauteren, I., Vanderauwera, S., Vandepoele, K., De Jaeger, G., Van Der Straeten, D. et al. (2013). ERF115 controls root quiescent center cell division and stem cell replenishment. *Science* **342**, 860-863.

Hibara, K., Karim, M. R., Takada, S., Taoka, K., Furutani, M., Aida, M. and Tasaka, M. (2006). Arabidopsis CUP-SHAPED COTYLEDON3 regulates postembryonic shoot meristem and organ boundary formation. *Plant Cell* **18**, 2946-2957.

Ibanes, M., Fabregas, N., Chory, J. and Caño-Delgado, A. I. (2009). Brassinosteroid signaling and auxin transport are required to establish the periodic pattern of Arabidopsis shoot vascular bundles. *Proc. Natl. Acad. Sci. USA* **106**, 13630-13635.

Johnston, R., Wang, M., Sun, Q., Sylvester, A. W., Hake, S. and Scanlon, M. J. (2014). Transcriptomic analyses indicate that maize ligule development recapitulates gene expression patterns that occur during lateral organ initiation. *Plant Cell* **26**, 4718-4732.

Kagale, S. and Rozwadowski, K. (2011). EAR motif-mediated transcriptional repression in plants: an underlying mechanism for epigenetic regulation of gene expression. *Epigenetics* **6**, 141-146.

Kagale, S., Links, M. G. and Rozwadowski, K. (2010). Genome-wide analysis of ethylene-responsive element binding factor-associated amphiphilic repression motif-containing transcriptional regulators in Arabidopsis. *Plant Physiol.* **152**, 1109-1134.

Ke, J., Ma, H., Gu, X., Thelen, A., Brunzelle, J. S., Li, J., Xu, H. E. and Melcher, K. (2015). Structural basis for recognition of diverse transcriptional repressors by the TOPLESS family of corepressors. *Sci. Adv.* **1**, e1500107.

Kieffer, M., Stern, Y., Cook, H., Clerici, E., Maulbetsch, C., Laux, T. and Davies, B. (2006). Analysis of the transcription factor WUSCHEL and its functional homologue in Antirrhinum reveals a potential mechanism for their roles in meristem maintenance. *Plant Cell* **18**, 560-573.

Krogan, N. T., Hogan, K. and Long, J. A. (2012). APETALA2 negatively regulates multiple floral organ identity genes in Arabidopsis by recruiting the co-repressor TOPLESS and the histone deacetylase HDA19. *Development* **139**, 4180-4190.

Kwon, C. S., Hibara, K.-I., Pfluger, J., Bezhani, S., Metha, H., Aida, M., Tasaka, M. and Wagner, D. (2006). A role for chromatin remodeling in regulation of CUC gene expression in the Arabidopsis cotyledon boundary. *Development* **133**, 3223-3230.

Laufs, P., Peaucelle, A., Morin, H. and Traas, J. (2004). MicroRNA regulation of the CUC genes is required for boundary size control in Arabidopsis meristems. *Development* **131**, 4311-4322.

Lee, J., He, K., Stolc, V., Lee, H., Figueroa, P., Gao, Y., Tongprasit, W., Zhao, H., Lee, I. and Deng, X. W. (2007). Analysis of transcription factor HY5 genomic binding sites revealed its hierarchical role in light regulation of development. *Plant Cell* **19**, 731-749.

Lee, H.-S., Kim, Y., Pham, G., Kim, J. W., Song, J.-H., Lee, Y., Hwang, Y.-S., Roux, S. J. and Kim, S.-H. (2015). Brassinazole resistant 1 (BZR1)-dependent brassinosteroid signalling pathway leads to ectopic activation of quiescent cell division and suppresses columella stem cell differentiation. *J. Exp. Bot.* **66**, 4835-4849.

Li, Q.-F., Wang, C., Jiang, L., Li, S., Sun, S. S. M. and He, J.-X. (2012). An interaction between BZR1 and DELLAs mediates direct signaling crosstalk between brassinosteroids and gibberellins in Arabidopsis. *Sci. Signal.* **5**, ra72.

Long, J. A., Ohno, C., Smith, Z. R. and Meyerowitz, E. M. (2006). TOPLESS regulates apical embryonic fate in Arabidopsis. *Science* **312**, 1520-1523.

Lozano-Durán, R., Macho, A. P., Boutrot, F., Segonzac, C., Somssich, I. E. and Zipfel, C. (2013). The transcriptional regulator BZR1 mediates trade-off between plant innate immunity and growth. *Elife* **2**, e00983.

Nakagawa, T., Kurose, T., Hino, T., Tanaka, K., Kawamukai, M., Niwa, Y., Toyooka, K., Matsuoka, K., Jinbo, T. and Kimura, T. (2007). Development of series of gateway binary vectors, pGWBs, for realizing efficient construction of fusion genes for plant transformation. *J. Biosci. Bioeng.* **104**, 34-41.

Oh, E., Zhu, J.-Y. and Wang, Z.-Y. (2012). Interaction between BZR1 and PIF4 integrates brassinosteroid and environmental responses. *Nat. Cell Biol.* **14**, 802-809.

Oh, E., Zhu, J. Y., Ryu, H., Hwang, I. and Wang, Z. Y. (2014). TOPLESS mediates brassinosteroid-induced transcriptional repression through interaction with BZR1. *Nat. Commun.* **5**, 4140.

Pauwels, L., Barbero, G. F., Geerinck, J., Tilleman, S., Grunewald, W., Pérez, A. C., Chico, J. M., Bossche, R. V., Sewell, J., Gil, E. et al. (2010). NINJA connects the co-repressor TOPLESS to jasmonate signalling. *Nature* **464**, 788-791.

Reddy, G. V., Heisler, M. G., Ehrhardt, D. W. and Meyerowitz, E. M. (2004). Real-time lineage analysis reveals oriented cell divisions associated with morphogenesis at the shoot apex of Arabidopsis thaliana. *Development* **131**, 4225-4237.

Ryu, H., Cho, H., Bae, W. and Hwang, I. (2014). Control of early seedling development by BES1/TPL/HDA19-mediated epigenetic regulation of ABI3. *Nat. Commun.* **5**, 4138.

Sablowski, R. (2007). Flowering and determinacy in Arabidopsis. *J. Exp. Bot.* **58**, 899-907.

Sun, Y., Fan, X.-Y., Cao, D.-M., Tang, W., He, K., Zhu, J.-Y., He, J.-X., Bai, M.-Y., Zhu, S., Oh, E. et al. (2010). Integration of brassinosteroid signal transduction with the transcription network for plant growth regulation in Arabidopsis. *Dev. Cell* **19**, 765-777.

Szemenyei, H., Hannon, M. and Long, J. A. (2008). TOPLESS mediates auxin-dependent transcriptional repression during Arabidopsis embryogenesis. *Science* **319**, 1384-1386.

Takada, S., Hibara, K., Ishida, T. and Tasaka, M. (2001). The CUP-SHAPED COTYLEDON1 gene of Arabidopsis regulates shoot apical meristem formation. *Development* **128**, 1127-1135.

Tao, Q., Guo, D., Wei, B., Zhang, F., Pang, C., Jiang, H., Zhang, J., Wei, T., Gu, H., Qu, L.-J. et al. (2013). The TIE1 transcriptional repressor links TCP transcription factors with TOPLESS/TOPLESS-RELATED corepressors and modulates leaf development in Arabidopsis. *Plant Cell* **25**, 421-437.

Tian, C., Zhang, X., He, J., Yu, H., Wang, Y., Shi, B., Han, Y., Wang, G., Feng, X., Zhang, C. et al. (2014). An organ boundary-enriched gene regulatory network uncovers regulatory hierarchies underlying axillary meristem initiation. *Mol. Syst. Biol.* **10**, 755.

Truernit, E. and Haseloff, J. (2008). A simple way to identify non-viable cells within living plant tissue using confocal microscopy. *Plant Methods* **4**, 15.

Vert, G., Nemhauser, J. L., Geldner, N., Hong, F. and Chory, J. (2005). Molecular mechanisms of steroid hormone signaling in plants. *Annu. Rev. Cell Dev. Biol.* **21**, 177-201.

Vilarrasa-Blasi, J., González-García, M.-P., Frigola, D., Fàbregas, N., Alexiou, K. G., López-Bigas, N., Rivas, S., Jauneau, A., Lohmann, J. U., Benfey, P. N. et al. (2014). Regulation of plant stem cell quiescence by a brassinosteroid signaling module. *Dev. Cell* **30**, 36-47.

Vroemen, C. W., Mordhorst, A. P., Albrecht, C., Kwaaitaal, M. A. and de Vries, S. C. (2003). The CUP-SHAPED COTYLEDON3 gene is required for boundary and shoot meristem formation in Arabidopsis. *Plant Cell* **15**, 1563-1577.

Wang, Z.-Y., Bai, M.-Y., Oh, E. and Zhu, J.-Y. (2012). Brassinosteroid signaling network and regulation of photomorphogenesis. *Annu. Rev. Genet.* **46**, 701-724.

Wang, L., Kim, J. and Somers, D. E. (2013). Transcriptional corepressor TOPLESS complexes with pseudoresponse regulator proteins and histone deacetylases to regulate circadian transcription. *Proc. Natl. Acad. Sci. USA* **110**, 761-766.

Wang, L., Wang, B., Jiang, L., Liu, X., Li, X., Lu, Z., Meng, X., Wang, Y., Smith, S. M. and Li, J. (2015). Strigolactone signaling in Arabidopsis regulates shoot development by targeting D53-Like SMXL repressor proteins for ubiquitination and degradation. *Plant Cell* **27**, 3128-3142.

Yadav, R. K., Perales, M., Gruel, J., Girke, T., Jonsson, H. and Reddy, G. V. (2011). WUSCHEL protein movement mediates stem cell homeostasis in the Arabidopsis shoot apex. *Genes Dev.* **25**, 2025-2030.

Yin, Y., Vafeados, D., Tao, Y., Yoshida, S., Asami, T. and Chory, J. (2005). A new class of transcription factors mediates brassinosteroid-regulated gene expression in Arabidopsis. *Cell* **120**, 249-259.

Yu, H. and Huang, T. (2016). Molecular mechanisms of floral boundary formation in Arabidopsis. *Int. J. Mol. Sci.* **17**, 317.

Yu, X., Li, L., Zola, J., Aluru, M., Ye, H., Foudree, A., Guo, H., Anderson, S., Aluru, S., Liu, P. et al. (2011). A brassinosteroid transcriptional network revealed by genome-wide identification of BESI target genes in Arabidopsis thaliana. *Plant J.* **65**, 634-646.

Žádníková, P. and Simon, R. (2014). How boundaries control plant development. *Curr. Opin. Plant Biol.* **17**, 116-125.

Zhang, D., Jing, Y., Jiang, Z. and Lin, R. (2014). The chromatin-remodeling factor PICKLE integrates brassinosteroid and gibberellin signaling during skotomorphogenic growth in Arabidopsis. *Plant Cell* **26**, 2472-2485.

Zhu, Z., Xu, F., Zhang, Y., Cheng, Y. T., Wiermer, M., Li, X. and Zhang, Y. (2010). Arabidopsis resistance protein SNC1 activates immune responses through association with a transcriptional corepressor. *Proc. Natl. Acad. Sci. USA* **107**, 13960-13965.

DEVELOPMENT